Available online at www.banglajol.info

Bangladesh J. Sci. Ind. Res. **49(2)**, 103-110, 2014

BANGLADESH JOURNAL OF SCIENTIFIC AND INDUSTRIAL RESEARCH

E-mail: bjsir07@gmail.com

BCSIR

Angle resolver X-ray photoelectron spectroscopic analysis of the passive film of the corrosion-resistant W-32Zr alloy in 12 M HCl solution

Jagadeesh Bhattarai*

Central Department of Chemistry, Tribhuvan University, Kirtipur, Kathmandu, Nepal.

Abstract

The sputter-deposited amorphous W-32Zr alloy was passivated spontaneously and showed a fairly high corrosion resistance in 12 M HCl solution in open air at 30°C. The average corrosion rate of the W-32Zr alloy (i.e., 5.2×10^{-3} mm/y) was found to be lower than those of alloy-constituting tungsten and zirconium elements. Such synergistic effects of simultaneous addition of tungsten and zirconium in the W–32Zr alloy was investigated by corrosion tests, electrochemical measurements and angle resolved X-ray photoelectron spectroscopic (ARXPS) analyses. High corrosion resistance of the binary W–32Zr alloy is mostly due to the formation of homogeneous passive oxyhydroxide film consisting of W^{ox} and Zr^{4+} cations with a small concentration gradient in–depth from ARXPS analysis. Consequently, zirconium metal acts synergistically with tungsten in enhancing the anodic passivity as well as the corrosion resistance properties of the sputter–deposited W–32Zr alloy in 12 M HCl solution open to air at 30°C.

Keywords: W–32Zr alloy; Corrosion resistance; Sputter deposition; In–depth analysis; Take–off angle of photoelectrons

Introduction

Angle resolved X-ray photoelectron spectroscopic (ARXPS) technique is one of the advanced and more precise techniques for thin surface analyses in wide fields of materials sciences. During the last five decades, it becomes a very useful surface analytical tool for corrosion scientists to study the mechanism of high corrosion resistance property of materials and their anodic passivity after a valuable contribution of K. Siegbahn and his research group (Siegbahn *et al.* 1967). It is widely used by a number of researchers to gain about in–depth concentration profiles of thin films. ARXPS proves as one of the promising thin surface analysis techniques to investigate the chemical compositions, oxidation states, chemical shifts and electronic properties of the thin films (Harris 1969; Fraser *et al.* 1973; Fadley 1974; Fadley and Baird 1974; Baird and Fadley 1977; Pijolat and Hollinger 1981; Tougaard and Ignatiev 1983). In principle, the in–depth information of the thin films depends on the effective escape depth of the ejected photoelectrons, which increases with an increase in the take–off angle of photoelectrons relative to the surface of the sample specimen (Harris 1969; Fraser *et al.* 1973; Fadley 1974; Fadley and Baird 1974; Baird and Fadley 1977; Pijolat and Hollinger 1981; Tougaard and Ignatiev 1983; Akiyama *et al.* 1996). The surface sensitivity is varied by changing the take–off angle of photoelectrons in the ARXPS technique (Fadley and Baird 1974; Bhattarai 2011 a). At a lower take–off angle of photoelectrons, the intensity signals (I) from the surface of sample species located in the exterior part of the surface films are enhanced. Therefore, the apparent composition of the surface films is changed with the take–off angle of photoelectrons in the ARXPS measurements (Bhattarai 2012). In recent years, this ARXPS technique was used to examine the formation of homogeneous orheterogeneous nature of the passive films formed on the corrosion–resistant alloys (Asami *et al.* 1987; Akiyama *et al.* 1996; Bhattarai *et al.* 1998 a, 1998 b, 1998 c; Marcus 1998; Bhattarai 1998, 2000, 2010 a).

The sputter–deposited alloys consisting of either amorphous or nanocrystalline phases are chemically homogeneous and hence are interesting in the view of corrosion resistance property as well as the passivity (Hashimoto 1993). The passivating elements such as tungsten and zirconium can generally improve corrosion resistance of alloys in aggressive environments. It has been reported that less than 10 at% (atomic percentage) of tungsten addition to sputter–deposited W–xCr alloys was enough to cause spontaneous passivation of the alloys and they showed higher corrosion resistance than those of tungsten and chromium in aggressive environments (Bhattarai *et al.* 1998 c; Bhattarai 1998, 2000; Basnet and Bhattarai 2010). On the other hand, zirconium is widely known for its superior corrosion resistance behavior in acidic environments, although it suffers pitting corrosion by anodic polarization. The alloying of zirconium with aluminum (Yoshioka *et al.* 1991), chromium (Kim *et al.* 1993; Li *et al.*

*Corresponding authors: E-mail: bhattatai_05@yahoo.com

1997; Mehmood *et al.* 1998), molybdenum (Park *et al.* 1995; Hashimoto *et al.* 2007) and tungsten (Bhattarai *et al.* 1997; Shrestha and Bhattarai 2010) greatly improved the corrosion resistance properties of the binary sputter–deposited alloys in aggressive environments. The immunity to passivity breakdown like the pitting corrosion is one of the most interesting characteristics of the zirconium containing alloys. It has been reported that the synergistic improvement in the resistance to the passivity breakdown of the alloys in chloride–containing aggressive environments was reported when simultaneous additions of tungsten, zirconium, chromium or nickel to the sputter–deposited ternary W–xZr–yCr (Aryal and Bhattarai 2010, 2011; Kumal and Bhattarai 2010; Bhattarai 2010 b, 2011 b, 2011 c) or W–xCr–yNi (Bhattarai 2009; Bhattarai and Kharel 2009–10; Kharel and Bhattarai 2009; Bhattarai 2010 a) alloys instead of single addition of zirconium, chromium or nickel metals. The synergistic improvement in the resistance to corrosion as well as the pitting corrosion of these sputter–deposited binary and ternary tungsten-based alloys was attributed to the formation of double oxyhydroxide passive films of the alloy–constituting elements from the XPS analyses. In this context, the present work is aimed to clarify the mechanism of the higher corrosion resistance of the sputter–deposited amorphous W–32Zr alloy than those of tungsten and zirconium metals in 12 M HCl solution open to air at 30°C using angel resolved XPS technique.

Materials and methods

The sputter–deposited W–32Zr alloy was characterized as an amorphous single–phase solid having an apparent grain size of about 2 nm from the most intense XRD peak using Scherrer's formula (Cullity 1977) which was reported elsewhere (Bhattarai *et al.* 1997). The composition of the alloy hereafter is denoted in atomic percentage (at %).

Prior to the corrosion tests, electrochemical measurements and angle resolved XPS analyses, the sputter–deposited W–32Zr alloy specimens were mechanically polished with a silicon carbide paper up to grit number 1500 in cyclohexane, degreased by acetone and dried in air. The average corrosion rate of the alloy was estimated using weight loss method after immersion for 168 h in 12 M HCl solution open to air at 30°C.

The composition of the passive film of the W-32Zr alloy was analyzed by XPS including angle–resolved measurements. Before and after immersion in 12 M HCl solution, XPS spectra were measured by a Shimadzu ESCA–850 photoelectron spectrometer with Mg Kα (hν = 1253.6 eV) radiation for surface analyses including the in–depth distribution of the species in the surface of the W-32Zr alloy. XPS spectra for the W–32Zr alloy over a wide binding energy region (i.e., 0–1000 eV) exhibited peaks of tungsten, zirconium, carbon, oxygen and chlorine. The most intense peaks of the W 4f, Zr 3d, C 1s, O 1s and Cl 2p electrons were measured in the binding energy range of 20 eV for all spectra. For the alloy specimen immersed in 12 M HCl solution, the Cl 2p spectrum was detected at about 199.0 eV, which comes from chloride ions. However, the intensity of the Cl 2p peak was very low and hence the concentration of the chloride ions was not considered in the calculation. The O 1s spectrum was composed of two peaks; the lower binding energy peak at 530.4 eV was assigned to OM oxygen, and the higher binding energy peak at 532.3 eV was assigned to OH oxygen (Asami and Hashimoto 1977). The spectra from the alloy constituents indicated the presence of the oxidized and metallic species; the former comes from the surface film and the latter from the underlying alloy surface. The measured spectra of W 4f and Zr 3d electrons were separated into W^{ox} 4f and W^{o} 4f; Zr^{4+} 3d and Zr^{o} 3d, respectively. The superscripts, "ox", 4+ and 0 denoted oxidized, tetravalent and metallic states, respectively. Furthermore, the W^{o} 4f spectrum was consisted of lower and higher binding energy peaks corresponding to W^{o} 4f7/2 and W^{o} 4f5/2 electrons. Similarly, the W^{ox} 4f spectrum was also composed of three doublets of the overlapped spectra of three oxidized species, that is, doublets of W^{4+} 4f7/2 and W^{4+} 4f5/2 ; W^{5+} 4f7/2 and W^{5+} 4f5/2 ; and W^{6+} 4f7/2 and W^{6+} 4f5/2 electrons. The peak binding energies of each peak were further corrected using the energy value of 285 eV for C 1s electronic state. The integrated intensities of the W^{o} 4f, W^{4+} 4f, W^{5+} 4f, W^{6+} 4f, Zr^{o} 3d, and Zr^{4+} 3d were obtained by the same method as those described elsewhere (Asami 1976; Asami and Hashimoto 1977; Bhattari *et al.* 1997).

The quantitative determination was performed under the assumption of a three–layer model: the outermost contaminant hydrocarbon layer of uniform thickness, the surface film of uniform thickness, and the underlying alloy surface of X–ray photoelectron spectroscopically infinite thickness, along with the assumption of homogenous distribution of the constituents in each layer. For angle–resolved XPS, the angle between the specimen surface and the direction of photoelectron to the detector (take–off angle of photoelectrons) was changed by using tilted–specimen holders at 30°, 45°, 60° and 90°. The photo–ionization cross–section of the W 4f and Zr 3d electrons relative to the O 1s electrons used were 2.97 (Kawashima *et al.* 1984) and 2.561 (Scofield 1978), respectively.

Results and discussion

Corrosion behavior of the sputter–deposited W–32Zr alloy

The corrosion rates of the sputter–deposited W–32Zr alloy and alloy–constituting elements were estimated from weight losses after immersion for 168 hours in 12 M HCl solution

open to air at 30°C. The weight loss for each specimen was estimated two times or more and the average corrosion rate was calculated. Figure 1 shows the corrosion rates of the sputter–deposited amorphous W–32Zr alloy including the sputter–deposited tungsten and zirconium metals after immersion for 168 h in 12 M HCl solution open to air at 30°C. The average corrosion rates of the tungsten and zirconium are 2.76×10^{-2} mm/y and 9.19×10^{-3} mm/y, respectively, in 12 M HCl. By contrast, the W–32Zr alloy shows even lower corrosion rate (i.e., 5.20×10^{-3} mm/y) than those of alloy–constituting elements (i.e., tungsten and zirconium). These results reveal that the corrosion resistance of the W-32Zr alloy is surprisingly improved in 12 M HCl solution open to air at 30°C. Consequently, it can be said that both tungsten and zirconium improve the corrosion resistance of the sputter–deposited W–32Zr alloy synergistically. Such synergistic effect of the simultaneous additions of tungsten and zirconium has been reported for other sputter–deposited W–xZr alloys due to the formation of the double oxyhydroxides of tungsten and zirconium in 12 M HCl solution from the conventional XPS analyses (Bhattarai *et al.* 1997; Bhattarai 1998).

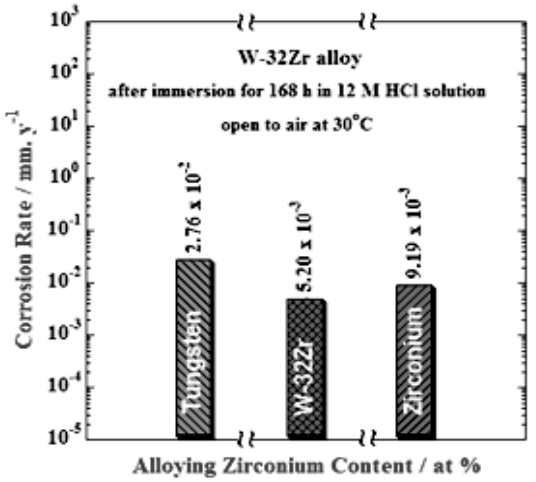

Fig. 1. The corrosion rates of the sputter–deposited W–32Zr alloy including the sputter–deposited tungsten and zirconium metals after immersion for 168 h in 12 M HCl solution open to air at 30°C.

Take–off angle dependence of the surface composition of the W–32Zr alloy

The corrosion rate of the sputter–deposited binary W–32Zr alloy is about nearly one order of magnitude lower than that of tungsten and even lower than that of zirconium in 12 M HCl solution as discussed above in Fig. 1. The experimental results of the angle resolved XPS measurements are presented here to clarify the mechanism of such higher corrosion resistance behavior of the sputter–deposited binary W–xZr alloys than those of alloy–constituting elements in 12 M HCl. Because, the in–depth surface analyses of the spontaneously passivated double oxyhydroxide films formed on the W–xZr alloys using angle resolved XPS measurements give very important information for a better understanding of the effects of the simultaneous additions of tungsten and zirconium additions in the corrosion–resistant properties as well as in the passivity of the alloys.

An information about indepth composition change of the passive film formed on the sputter–deposited W–32Zr alloy was obtained by a non–destructive depth profiling technique of the angle resolved XPS to know whether the spontaneously passivated film of W-32Zr alloy is homogeneous or not. Figures 2 and 3 show the deconvolution of the W 4f and Zr 3d spectra, respectively, measured for the sputter–deposited W–32Zr alloy after immersion for 18 hours in 12 M HCl solution at 30°, 60° and 90° take–off angle of photoelectrons. The measured spectra for the W 4f and Zr 3d electrons are separated into W° 4f and W^{ox} 4f, and Zr° 3d and Zr^{4+} 3d state spectra, respectively. The doublets of W° 4f and Zr° 3d spectra are assigned to the metallic state of tungsten and zirconium, respectively, in the surfaces. The W^{ox} 4f spectrum is composed of three doublets of the overlapped spectra of three oxidized species of W^{6+}, W^{5+} and W^{4+} ions. The integrated intensities of these all spectra were separately obtained by the same method as that described elsewhere (Asami 1976; Asami and Hashimoto 1977; Bhattarai 1998).

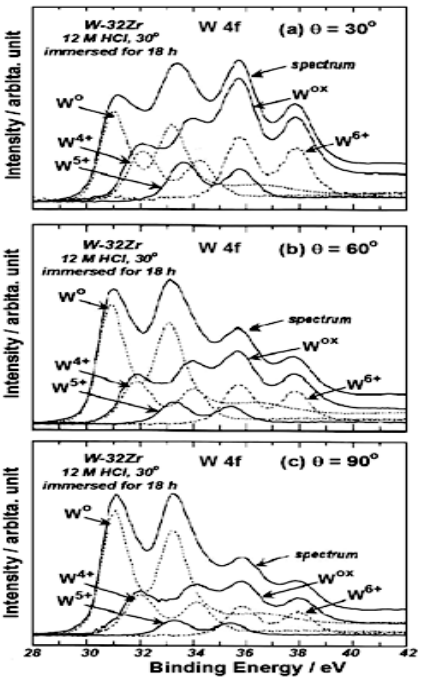

Fig. 2. Deconvolution of the W 4f spectra measured for the W-32Zr alloy at different take-off angle of photoelectrons in the given conditions.

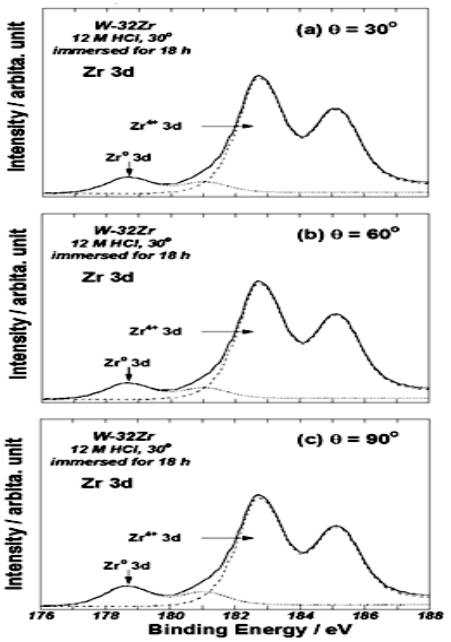

Fig. 3. Deconvolution of the Zr 3d spectra measured for the W-32Zr alloy at different take-off angle of photoelectrons in the given conditions.

The in−depth compositional changes in the surfaces of the sputter−deposited W−32Zr alloy were analyzed using angle resolved XPS. Figures 4 (a) and 5 (b) show the changes in apparent cationic fractions in the airformed film as well as the spontaneously passivated films and apparent atomic fractions in the underlying alloy surfaces, respectively, for the sputter−deposited W−32Zr alloy as a function of take−off angle of photoelectrons. The figures clearly revealed that zirconium is concentrated in air−formed oxide films of the alloy as a result of preferential oxidation of zirconium, while tungsten is significantly concentrated in the passive films of the alloy after immersion for 1−168 hours in 12 M HCl solution open to air at 30°C. There is some concentration gradient of tungsten and zirconium in both the air−formed oxide film and the spontaneously formed passive film formed on the W−32Zr alloy by exposing to air after mechanical polishing and after immersion for different periods of time in 12 M HCl at 30°C, respectively. Zirconium is increased almost linearly with take−off angle of photoelectrons. In particular, the concentration of zirconium ion is slightly higher in the interior part (i.e., at take−off angle of 90°) of the zirconium−rich passive film formed on the W−32Zr alloy.

On the other hand, the concentration of tungsten is slightly higher in the exterior part (i.e., at take−off angle of 30°) of the underlying alloy surface and hence the tungsten concentration decreased with take−off angle of photoelectrons. Consequently, the synergistic effect of tungsten and zirconium additions on the W−32Zr alloy is explained and hence it showed higher corrosion resistance than those of tungsten and zirconium even in very aggressive 12 M HCl

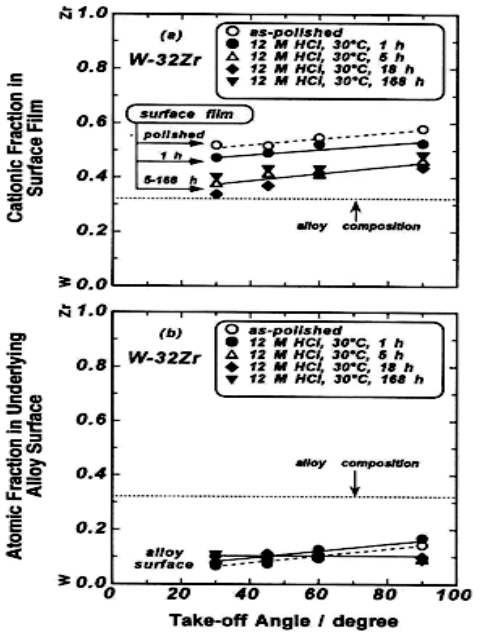

Fig. 4. Changes in the (a) apparent cationic fractions in the surface films and (b) atomic fractions in the underlying alloy surface of the W-32Zr alloy as a function of take-off angles.

solution at 30°C. Figure 5 shows a diagrammatic sketch of a model of the surfaces of the sputter−deposited W−32Zr alloy in which the concentration of tungsten and zirconium are slightly changed with depth in both spontaneously passivated surface film and the underlying alloy surface.

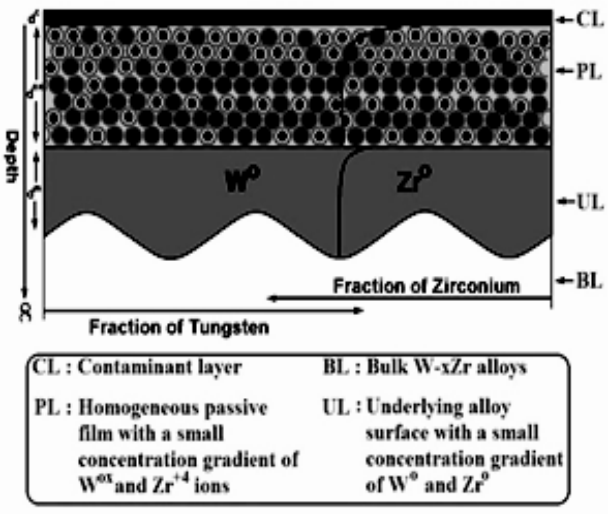

Fig. 5. A model of the surface of the W-32Zr alloy in which there is a small indepth concentration gradients of tungsten and zirconium in both the spontaneously passivated film and the underlying alloy surface.

For a better understanding of the role of tungsten ions in the passive film formed on the W-32Zr alloy, the changes in the ratios of W^{4+}, W^{5+} and W^{6+} ions in the surface film was determined quantitatively. Figure 6 shows the concentration ratios of W^{4+}, W^{5+} and W^{6+} ions to the total tungsten ions (W^{ox}) in the spontaneously passivated film of the W–32Zr alloy after immersion for 1 and 18 hours in 12 M HCl solution open to air at 30°C, as a function of take–off angle of photoelectrons. The ratio of W^{6+} ions in the passive film of the W–32Zr alloy is significantly higher than those of W^{4+} and W^{5+} ions in the films. The W^{6+} ion decreases with increasing take–off angle of photoelectrons, while W^{4+} ion increases with take–off angles. The ratio of W^{5+} ion remains almost constant with take–off angles. Accordingly, the W^{4+} ion is particularly concentrated in the interior (i.e., at take–off angle of 30°) of the spontaneously passivated film formed on the W–32Zr alloy, while the concentration of W^{6+} ion is higher in the exterior (at take–off angle of 90°) of the passive film. It is generally known that air exposure of the specimen during transfer from the electrolyte to the XPS analyzing chamber give rise to oxidation of W^{4+} to W^{6+} ion. Accordingly the relative ratio of W^{6+} ion is higher in the exterior of the surface films and decreased with the depth of the passive film.

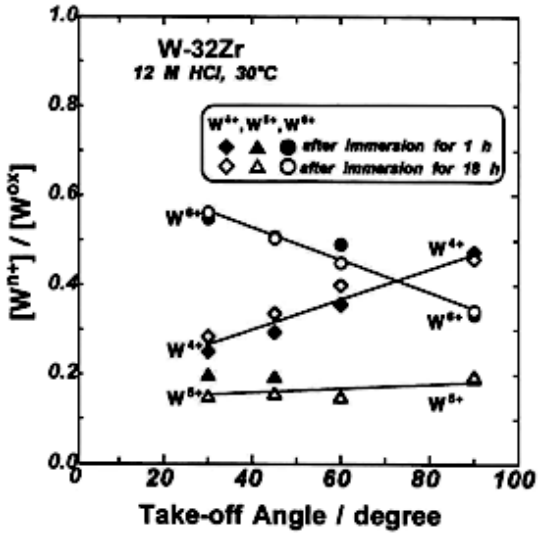

Fig. 6. The concentration ratios of W^{4+}, W^{5+} and W^{6+} ions to the total tungsten ions in the passive film formed on the W-32Zr alloy after immersion for different period of times in 12 M HCl as a function of take-off angle of photoelectrons.

In general, one of the characteristic of the passive films of the alloys is the concentration of oxygen species in the spontaneously passivated films formed on the corrosion–resistant alloys. Figure 7 shows the deconvolution of the O 1s spectra measure for the sputter–deposited W–32Zr alloy at 30°, 60° and 90° take–off angle of photoelectrons after immersion for 18 hours in 12 M HCl solution open to air at 30°C. The passive film formed on the spontaneously passivated W32Zr alloy consists of oxyhydroxide in which

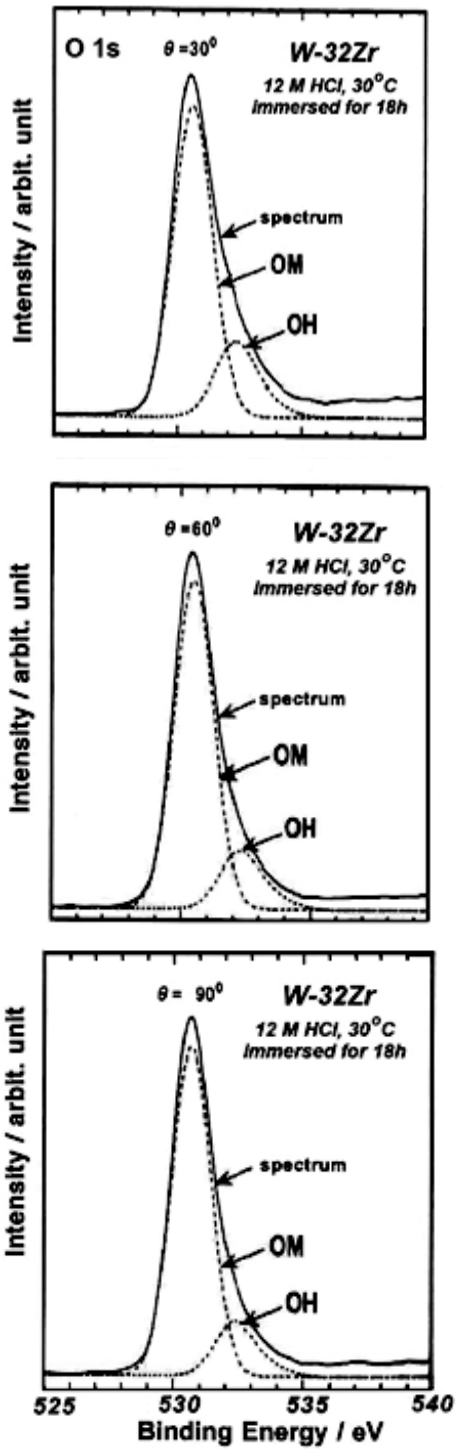

Fig. 7. Deconvolution of O 1s spectra measured for the W-32Zr alloy at different take-off angle of photoelectrons in the given conditions.

O^{2-} ion is a major oxygen species, although the OH peak corresponding to OH^- ion and bound H2O at low take–off angle of photoelectrons (i.e., at 30° of take–off angle of photoelectrons) is remarkably higher than that at high take–off angle of photoelectrons (i.e., at 90° take–off angle).

Figure 8 shows the changes in the ratios of [O^{2-}]/[cations] and [OH]/[cations] in the passive film of the W–32Zr alloy after immersion for different periods of time in 12 M HCl solution, as a function of take–off angle of photoelectrons. The ratios of [O^{2-}]/[cations] increase with the take–off angles and the ratios of [OH]/[cations] decrease with take–off angles in the alloy. The results reveal that the interior part of the passive film of the binary W–32Zr alloy is rather dry and well developed by MO–M bridging, while the exterior part of the passive film of the alloy is slightly wet with OH^- ion and H2O.

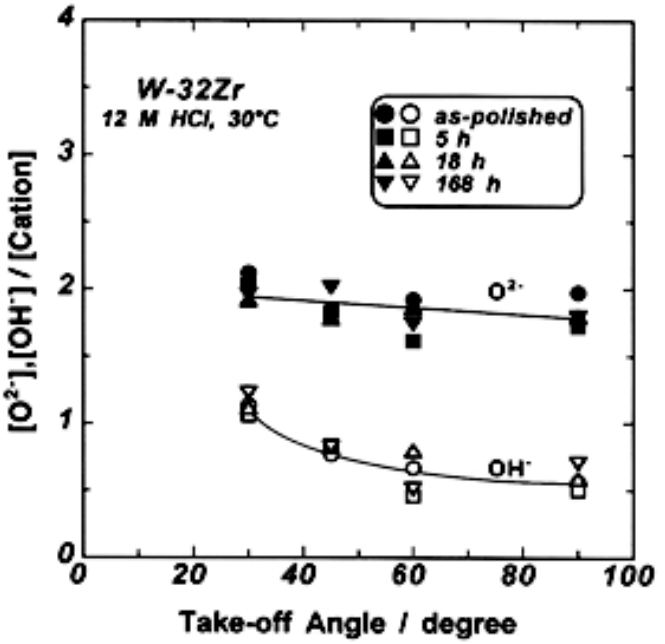

Fig. 8. shows the changes in the ratios of [O2-]/[cations] and [OH]/[cations] in the passive film of the W-32Zr alloy after immersion for different periods of time in 12 M HCl solution, as a function of take-off angle of photoelectrons.

Conclusion

The mechanism of the synergistic effect of tungsten and zirconium elements enhancing the higher corrosion resistance of the sputter–deposited amorphous W–32Zr alloy than those of alloying–constituting elements was studied using corrosion tests, electrochemical measurements and angle resolved XPS analyses in 12 M HCl solution open to air at 30°C. The following conclusions are drawn:

1. The sputter–deposited amorphous W–32Zr alloy is passivated spontaneously and hence it showed higher corrosion resistance than those of alloy–constituting elements.

2. The angle–resolved XPS analyses revealed that all cations of the binary alloy are distributed homogeneously in the films formed on spontaneously passivated alloy. The higher corrosion resistance of the alloy than those of the alloy–constituting elements is mostly due to the formation of the homogeneous passive films composed of both W^{4+} and Zr^{4+} ions with a small concentration gradient in–depth.

3. The W^{4+} ion is particularly concentrated in the interior of the spontaneously passivated film formed on the W–32Zr alloy, while the concentration of W^{6+} ion is higher in the exterior of the passive film.

4. The interior part of the passive film of the binary W–32Zr alloy is rather dry and well developed by M–O–M bridging, while the exterior part of the passive film of the alloy is slightly wet with OH^- ion and H2O.

Acknowledgement

Author is very thankful to Professors Emeritus; Dr. Koji Hashimoto and Dr. K. Asami of Tohoku University, Sendai, Japan for their heartful help and discussion on the ARXPS analyses.

References

Akiyama E, Kawashima A, Asami K and Hashimoto K 1996. A study of the structure of a passive film using angle–resolved x–ray photoelectron spectroscopy. *Corros. Sci.* **38**: 1127–1140.

Aryal BR and Bhattarai J 2010. Effects of alloying elements on the corrosion behavior of sputter–deposited Zr–(12–21)Cr–W alloys in 0.5 M NaCl solution. *J. Nepal Chem. Soc.* **25**: 75–82.

Aryal BR and Bhattarai J 2011. Effects of tungsten, chromium and zirconium on the corrosion behavior of ternary amorphous W–Cr–Zr alloys in 1 M NaOH solution. *Scientific World* **9**: 39–43.

Asami K 1976. A precisely consistent energy calibration method for X–ray photoelectron spectroscopy. *J. Electron Spectrosc. Relat. Phenom.* **9**: 469–478.

Asami K and Hashimoto K 1977. The X–ray photoelectron spectra of several oxides of iron and chromium. *Corros. Sci.* **17**: 559–570.

Asami K, De Sa MS and Ashworth V 1987. Influence of surface roughness on non–destructive in–depth analysis using angle resolved XPS and a method for its correction. *Boshoku Gijustsu* **36**: 621–626.

Baird RJ and Fadley CS 1977. X–ray photoelectron angular distributions with dispersion–compensating X–ray and electron optics. *J. Electron Spectrosc. Relat. Phenom.* **11**: 39–65.

Basnet M and Bhattarai J 2010. The corrosion behavior of sputter–deposited nanocrystalline W–Cr alloys in NaCl and NaOH solutions. *J. Nepal Chem. Soc.* **25**: 53–61.

Bhattarai J 1998. *Tailoring of corrosion-resistant tungsten alloys by sputtering*. Ph. D. thesis, Department of Materials Science, Faculty of Engineering, Tohoku University, Sendai, Japan. Pp. 229.

Bhattarai J 2000. A study of in–depth composition of the anodic passive films formed on the W–25Cr alloy by angle–resolved X–ray photoelectron spectroscopy. *J. Nepal Chem. Soc.* **19**: 1–14.

Bhattarai J 2009. The Effects of chromium and nickel on the passivation behavior of sputter–deposited W–Cr–Ni alloys in 12 M HCl solution. *Scientific World* **7**: 24–28.

Bhattarai J 2010 a. X–ray photoelectron spectroscopy analyses on the corrosion–resistant W–Cr–Ni alloys in 12 M HCl. *Trans. Mater. Res. Soc. Jpn*. **35(1)**: 1–6.

Bhattarai J 2010 b. The corrosion behavior of sputter–deposited ternary Zr–(12–18)Cr–W alloys in 12 M HCl solution. *J. Nepal Chem. Soc.* **26**: 13–21.

Bhattarai J 2011 a. *Introduction to electron spectroscopy for in-depth surface analysis*, 1st edition, Kathmandu, Nepal, 86 pp.

Bhattarai J 2011 b. Role of alloying elements on the corrosion behavior of sputter–deposited amorphous W–Cr–Zr alloys in 0.5 M NaCl solution. *Scientific World* **9**: 34–38.

Bhattarai J 2011 c. The corrosion behavior of sputter–deposited ternary W–Cr–(15–18)Zr alloys in 12 M HCl. *Afr. J. Pure Appl. Chem.* **5(8)**: 212–218.

Bhattarai J 2012. A non-destructive compositional analysis of thin surface films formed on W-xTa alloys by angle resolved x-ray photoelectron spectroscopy. *BIBECHANA* **8**: 8-16.

Bhattarai J, Akiyama E, Habazaki H, Kawashima A, Asami K and Hashimoto K 1997. Electrochemical and XPS studies of the corrosion behavior of sputter–deposited amorphous W–Zr alloys in 6 and 12 M HCl solutions. *Corros. Sci.* **39**: 353–375.

Bhattarai J, Akiyama E, Habazaki H, Kawashima A, Asami K and Hashimoto K 1998 a. Electrochemical and XPS studies of the corrosion behavior of sputter–deposited amorphous W–Nb alloys in concentrated hydrochloric acid solutions. *Corros. Sci.* **40**: 19–42.

Bhattarai J, Akiyama E, Habazaki H, Kawashima A, Asami K and Hashimoto K 1998 b. Electrochemical and XPS studies on the passivation behavior of sputter–deposited W–Cr alloys in 12 M HCl solution. *Corros. Sci.* **40**: 155–175.

Bhattarai J, Akiyama E, Habazaki H, Kawashima A, Asami K and Hashimoto K 1998 c. The passivation behavior of sputter–deposited W–Ta alloys in 12 M HCl. *Corros. Sci.* **40**: 757–779.

Bhattarai J and Kharel PL 2009–10. Effects of chromium and tungsten on the corrosion behavior of sputter–deposited W–Cr–Ni alloys in 0.5 M NaCl solution. *J. Inst. Sci. Technol.* **16**: 141–151.

Cullity BD 1977 in *Elements of X-ray Diffraction*, 2nd edition. Addison–Wesley Publ. Co. Inc., pp. 101–102.

Fadley CS and Baird RJ 1974. Surface analysis and angular distributions in X–ray photoelectron spectroscopy. *J. Electron Spectrosc. Relat. Phenom.* **5**: 93–137.

Fadley CS 1974. Instrumentation for surface studies: XPS angular distribution. *J. Electron Spectrosc. Relat. Phenom.* **5**: 725–754.

Fraser WA, Florio JV, Delgass WN and Robertson WD 1973. Surface sensitivity and angular dependence of X–ray photoelectron spectra. *Surf. Sci.* **36**: 661–674.

Harris LA 1969. Angular dependence in electron–excited angular emission. *Surf. Sci.* **15**: 77–93.

Hashimoto K 1993. Chemical properties of rapidly solidified alloy. in *Rapidly Solidified Alloys; Processes, Structures, Properties, Applications* (eds. Howard H. Liebermann), Marcel Dekker Inc., New York, p. 591–615.

Hashimoto K, Asami K, Kawashima A, Habazaki H and Akiyama E 2007. The role of corrosion–resistant alloying elements in passivity. *Corros. Sci.* **49**: 42–52.

Heusler K E and Huerta H 1988. in *Proc. Symposium on Corrosion, Electrochemistry and Catalysis of Metallic Glasses* (eds. R. B. Diegle and K. Hashimoto). The Electrochemical Soc., Pennington, p. 1.

Kawashima A, Asami K and Hashimoto K 1984. An XPS study of anodic behavior of amorphous nickel-phosphorus alloys containing chromium, molybdenum or tungsten in 1 M HCl. *Corros. Sci.* **24**: 807–812.

Kharel PL and Bhattarai J 2009. The corrosion behavior of sputter–deposited W–Cr–(4–15)Ni alloys in NaOH solutions. *J. Nepal Chem. Soc.* **24**: 3–11.

Kim JH, Akiyama E, Habazaki H, Kawashima A, Asami K and Hashimoto K 1993. The corrosion behavior of sputter–deposited amorphous chromium–zirconium alloys in 6 M HCl solution. *Corros. Sci.* **34**: 1817–1827.

Kumal RR and Bhattarai J 2010. Roles of alloying elements on the corrosion behavior of amorphous W–Zr–(15–33)Cr alloys in 1 M NaOH solution. *J. Nepal Chem. Soc.* **25**: 93–100.

Li XY, Akiyama E, Habazaki H, Kawashima A, Asami K and Hashimoto K 1997. An XPS study of passive films on corrosion–resistant Cr–Zr alloys prepared by sputter deposition. *Corros. Sci.* **39**: 1365–1380.

Marcus P 1998. Surface science approach of corrosion phenomena. *Electrochimica Acta* **1–2**: 109–118.

Mehmood M, Zhang BP, Akiyama E, Habazaki H, Kawashima A, Asami K and Hashimoto K 1998. Experimentally evidence for the critical size of heterogeneity areas for pitting corrosion of Cr–Zr alloys in 6 M HCl. *Corros. Sci.* **40**: 1–17.

Park PY, Akiyama E, Habazaki H, Kawashima A, Asami K and Hashimoto K 1995. The corrosion behavior of sputter–deposited amorphous Mo–Zr alloys in 12 M HCl. *Corros. Sci.* **37**: 307–320.

Pijolat M and Hollinger G 1981. New depth–profiling method by angular–dependent X–ray photoelectron spectroscopy. *Surf. Sci.* **105**: 114–128.

Scofield JH 1978. Hartree-Slater subshell photoionization cross-sections at 1254 and 1487 eV *J. Electron Spectrosc. Relat. Phenom.* **8**: 129-137.

Shrestha P and Bhattarai J 2010. The passivation behavior od sputter–deposited W–Zr alloys in NaCl and NaOH solutions. *J. Nepal Chem. Soc.* **25**: 37–45.

Siegbhahn K, Nordling C, Fahlman A, Nordberg RH, Hedman J, Johnssaon G, Bergmark T, Karlsson SE, Lindgren I and Lindberg B 1967. *ESSCA-Atomic, Molecular and Solid State Studied by Means of Electron Spectroscopy*, Almquist and Wiksells, Uppsal, Sweden.

Tougaard S and Ignatiev A 1983. Concentration depth profiles by XPS: a new approach. *Surf. Sci.* **129**: 355–365.

Yoshioka H, Habazaki H, Kawashima A, Asami K and Hashimoto K 1991. Anodic polarization behavior of sputter–deposited Al–Zr alloys in a neutral chloride–containing buffer solution. *Electrochemica Acta* **36(7)**: 1227–1233.

Received: 24 June 2013; Revised: 19 March 2014; Accepted: 3 June 2014.